

CONTENTS

Section	Page	
SUMMARY	1	1/A6
INTRODUCTION	1	1/A6
SYMBOLS	2	1/A7
SUBSURFACE OXIDATION TESTS	3	1/A8
RADIANT AND PLASMA ARCJET TEST DATA	4	1/A9
GAS CHEMISTRY AND FLOW DYNAMICS	7	1/A12
Effects of Gas Chemistry	7	1/A12
Effects of Flow Dynamics	8	1/A13
MASS LOSS CORRELATION	9	1/A14
CONCLUDING REMARKS	12	1/B3
REFERENCES	13	1/B4

item 230-4-15

NAS 1.60:1284

AUG 22 1978
NASA Technical Paper 1284

COMPLETED
ORIGINAL

Reinforced Carbon-Carbon Oxidation Behavior in Convective and Radiative Environments

Donald M. Curry, K. J. Johansen,
and Emily W. Stephens

AUGUST 1978

NASA

32

item 830-H-15
NASA 1284:1284

NASA Technical Paper 1284

Reinforced Carbon-Carbon Oxidation Behavior in Convective and Radiative Environments

Donald M. Curry

Lyndon B. Johnson Space Center, Houston, Texas

K. J. Johansen

Vought Corporation, Dallas, Texas

Emily W. Stephens

Lyndon B. Johnson Space Center, Houston, Texas



National Aeronautics
and Space Administration

**Scientific and Technical
Information Office**

1978

Blank Page

TABLES

Table		Page
I	RADIATIVE MASS LOSS CORRELATION DATA FOR 19-PLY BASELINE COATED RCC	14
II	CONVECTIVE MASS LOSS CORRELATION DATA FOR 19-PLY BASELINE COATED RCC	15

FIGURES

Figure		Page
1	Typical carbon-carbon substrate oxidation	16
2	Coated RCC mass loss as a function of exposure time	
	(a) At 1367 and 1459 K; 0.83, 0.91 and 1.01 kN/m ² . . .	17
	(b) At 1570 and 1589 K; 1.01, 1.62, and 1.72 kN/m ²	18
	(c) At 1256 K; 0.53 and 1.01 kN/m ²	19
	(d) At 1233 and 1256 K; 5.07 kN/m ²	20
	(e) At 1506, 1511, and 1536 K; 5.07 kN/m ²	21
	(f) At 1589, 1608, 1631, and 1639 K; 1.01, 2.43, 5.47, 6.67, and 7.60 kN/m ²	22
3	Typical RCC wing panel	23
4	Subsurface mass loss rate in a radiant environment . . .	24
5	Subsurface mass loss rate in a convective environment	25
6	Correlation of subsurface mass loss rates in radiative and convective environments	26

SUMMARY

Thermal testing of siliconized carbon-carbon to determine its oxidation characteristics when exposed to representative Space Shuttle entry environments has been performed in both radiant and convective (plasma arcjet) heating test facilities. A comparison of the measured mass loss from both test environments indicates a greater mass loss associated with the plasma arc testing. An assessment of this difference in mass loss in terms of the major differences between the two types of tests (gas chemistry and flow dynamics) was made and is discussed herein. Using the mass loss data obtained from exposing siliconized carbon-carbon in the plasma arcjet and radiant environments, suggested methods for making mission mass loss predictions are presented.

INTRODUCTION

Siliconized reinforced carbon-carbon (RCC) is used as the thermal protection system for the Space Shuttle Orbiter high-temperature wing leading edge and nose cap surfaces. The reinforced carbon-carbon system is capable of multimission reuse in Earth atmospheric ascent and entry environments; in addition, the RCC system maintains a smooth external surface while transmitting the aerodynamic loads to the nose cap forward bulkhead and to the wing spar through discrete mechanical attachments.

The RCC is an all-carbon composite formed from graphite cloth layers contained in a carbon matrix, the outer layers of which have been converted into silicon carbide (SiC), hereinafter referred to as coating, to prevent oxidation at elevated temperatures. Although the silicon carbide outer layers of the RCC act as a coating to prevent oxidation, mission life is limited either by coating erosion (i.e., surface recession of SiC) or by oxidation of the substrate below the coating, which results in diminished substrate strength and/or loss of coating adherence. To characterize the subsurface attack and its impact on RCC mission life, air oxidation tests were performed over a wide range of pressures and temperatures in plasma arcjets and radiant heating facilities (McGinnis, ref. 1). Microanalyses and mechanical property tests were also conducted by McGinnis to assess subsurface oxidation effects on RCC performance.

Medford (ref. 2) developed a model for predicting RCC oxidation performance, including chemical kinetics at the subsurface oxidation sites, diffusion of oxygen into the coating fissures, growth of product film on the coating external surface and fissure walls, and differential thermal expansion between coating and substrate. In a later publication (ref. 3), Medford extended his analysis to predict mass loss distribution within the carbon-carbon substrate. This distribution has an important effect on the RCC integrity in

1

terms of substrate load-carrying capability and coating/substrate interface adherence. In developing his analytical models, Medford used the experimental data from the RCC subsurface attack investigation by McGinnis (ref. 1) but did not distinguish between arcjet and radiant heating mass loss data. Stewart,¹ in comparing NASA Ames Research Center plasma arc mass loss data with radiant data at the same pressure and temperature conditions, noted that high mass loss was experienced when testing was performed in a plasma arcjet.

The external surfaces of the Space Shuttle Orbiter nose cap and wing leading edges are exposed to a convective environment, whereas the internal areas are subject to a radiant environment; therefore, this paper includes a comparison of coated RCC mass loss² when tested in radiant and convective environments for the purpose of setting guidelines for making mission mass loss predictions. Included in the paper are (1) a comparison of mass loss histories in radiant and plasma arcjet heating environments, (2) a discussion of the differences in gas chemistry and-flow dynamics between plasma arcjet and radiant testing and their effects on silicon carbide coating and on the carbon substrate oxidation, and (3) a comparison of a radiant environment mass loss correlation with a convective environment correlation.

As an aid to the reader, where necessary the original units of measure have been converted to the equivalent value in the Système International d'Unités (SI). The SI units are written first, and the original units are written parenthetically thereafter.

SYMBOLS

C_h	Stanton number for heat transfer
C_m	Stanton number for mass transfer
E	activation energy
K	reaction rate coefficient
K'	modified reaction rate coefficient
γ_K	elemental mass fraction
L_e	Lewis number

¹David A. Stewart (NASA Ames Research Center), personal communication, May 1975.

²The mass loss data discussed are for the coated RCC without tetraethyl orthosilicate (TEOS) impregnation; TEOS is a silica-producing liquid silicate which infiltrates the silicon carbide coating and the carbon substrate resulting in increased oxidation protection. The TEOS-impregnated RCC is used for the Space Shuttle Orbiter wing leading edge and nose cap.

\dot{M}_D	diffusion-rate-controlled mass loss
\dot{M}_R	reaction-rate-controlled mass loss
\dot{M}	subsurface mass loss rate
\dot{m}_d	diffusional mass flux
P	pressure
R	gas constant
T	temperature
u	velocity
γ	constant
ρ	density

Subscripts

1	coefficients derived from data for $T \leq 1367$ K
2	coefficients derived from data for $T > 1367$ K
e	boundary-layer edge
i	element
w	wall, heated surface

SUBSURFACE OXIDATION TESTS

Siliconized RCC is a life-limited material system designed to meet the multimission reuse requirements of the Space Shuttle Orbiter wing leading edge and nose cap. A series of RCC mass loss tests (ref. 1) was performed at three NASA plasma arc test facilities (Ames Research Center (ARC), Langley Research Center (LaRC), and Lyndon B. Johnson Space Center (JSC)) and at two radiant test facilities (Rockwell International, Space Division, radiant test facility and Vought mission cycle facility).³ The objectives of these tests were (1) to determine the effect of RCC temperature and pressure on subsurface attack and (2) to determine the differences, if any, between subsurface

³The plasma arcjet facility is designated as the convective environment and the radiant test facility as the radiant environment.

attack in a molecular environment (radiant) and a molecular/atomic environment (arcjet).

The plasma arcjet test conditions ranged in RCC temperature from 1089 K (1500° F) to 1756 K (2700° F) and in pressure from 1 kN/m² (0.01 atmosphere) to 10 kN/m² (0.10 atmosphere). The test specimens were discs (7.11 centimeters diameter by 0.66 centimeter thick) with a nominal area of 94.21 square centimeters (14.6 square inches). The radiant test conditions ranged in temperature from 811 K (1000° F) to 1700 K (2600° F) and in pressure from 1.01 kN/m² (0.01 atmosphere) to 13.38 kN/m² (0.132 atmosphere). The Rockwell radiant test specimens consisted of both 7.11-centimeter-diameter discs and rectangular bars (2.0 by 12.44 by 0.66 centimeters) with a nominal area of 69.70 square centimeters (10.80 square inches). The Vought mission cycle test specimens consisted also of 7.11-centimeter-diameter discs and rectangular bars (16.51 by 3.81 by 1.16 centimeters) with a nominal area of 172.77 square centimeters (26.78 square inches). The area values for both the plasma and the radiant test specimens include both sides plus edges, since it is assumed that the entire test specimen was subjected to the environment.

The life limit of the RCC material is a function of both surface coating erosion and subsurface oxidation. An example of carbon-carbon subsurface oxidation resulting from inherent microcracks in the silicon carbide coating is shown in the photomicrograph presented as figure 1. Oxidation of the substrate occurs when small amounts of oxygen penetrate the coating and react with the carbon matrix and fibers to decrease the strength of the substrate and the adherence of the coating. Structural performance of RCC after mass loss was determined by microanalyses and mechanical property tests including tension, compression, flexure, and in-plane shear measurements. For a given mass loss, the performance degradation of the RCC was the same whether caused by radiant or convective environments.

McGinnis (ref. 1) presents the experimental results associated with each specimen tested in the subsurface oxidation investigation. Basically, reference 1 provides the test and target values of temperature, pressure, heat flux and test duration, test comments, final mass loss, and final mass loss rates. The mass loss data presented in reference 1 have been summarized in tables I and II for use in comparing the radiant and plasma arc test results.

RADIANT AND PLASMA ARCJET TEST DATA

A comparison of mass loss histories for RCC specimens exposed to plasma arcjet and radiant heating environments at comparable temperature and pressure conditions, presented in this section, demonstrates the effect of the testing environment on mass loss. The data comparison will be used to justify separate mass loss rate correlations for each type of environment.

Figures 2(a) to 2(c) are comparisons of mass loss per area for specimens tested in the Rockwell radiant test facility and the JSC 10-megawatt plasma arc facility. Figure 2(a) is a comparison curve for specimens exposed at RCC temperatures of 1367 K (2000° F) and 1459 K (2165° F) and an approximate

pressure of 1.0 kN/m^2 (0.010 atmosphere). The mass loss measured after a 5-hour exposure in the plasma facility was significantly higher than the mass loss associated with the radiant test. Throughout the thermal exposure testing of the RCC, it was observed (ref. 1) that increases in the air pressure at the RCC surface at a given temperature resulted in a shorter mass gain duration and a greater final mass loss rate. It was also observed that the mass gain portion of the mass loss history is longer in duration for specimens exposed in a radiant environment than for those tested in a plasma arcjet environment. A comparison of the data for the two specimens tested at an RCC temperature of 1367 K illustrates the effect of the environment on the mass gain; the plasma-arc-tested specimen had a shorter mass gain period (approximately 30 minutes) than did the radiantly heated specimen (approximately 4 hours). Figure 2(a) also illustrates the combined effects of temperature and pressure on RCC subsurface mass loss for a specimen that gains little or no mass; the subsurface mass loss begins and continues at an approximately constant mass loss rate throughout the test.

After 5 hours exposure in the plasma facility, the specimen tested at 1459 K and 0.91 kN/m^2 had a mass loss of 0.0044 g/cm^2 , whereas the specimen tested at 1367 K and 0.83 kN/m^2 had a mass loss of 0.0017 g/cm^2 .

Figure 2(b) is a comparison of radiant and plasma arc test results at an RCC temperature of 1589 K (2400° F) and pressures of 1.01 kN/m^2 (0.010 atmosphere) and 1.62 kN/m^2 (0.016 atmosphere), respectively. Results for a second plasma arc specimen tested at a temperature of 1570 K and a pressure of 1.72 kN/m^2 also are presented. Data from the plasma-tested specimens indicate a shorter mass gain period ($\sqrt{3}$ hours) and approach a constant final mass loss slope, in contrast to the radiantly tested specimen, which appears to be reaching its maximum mass gain after 5 hours of exposure.

A comparison of mass loss for specimens exposed at a temperature of 1256 K (1800° F) and at a plasma test of 0.53 kN/m^2 (0.0052 atmosphere) and a radiant test pressure of 1.01 kN/m^2 (0.010 atmosphere) is shown in figure 2(c). Medford's analysis (refs. 2 and 3) of measured mass loss indicates that for pressures less than 10.1 kN/m^2 (0.10 atmosphere), the steady-state mass loss rate \dot{M} varies as a function of pressure P to the 0.8 power ($\dot{M} = f(P^{0.8})$). The data of figure 2(c) show an apparent effect of pressure on the mass loss, but pressure effects do not completely explain the difference in mass loss between radiantly and convectively tested specimens. However, a study of the radiant test data (table I) at 1256 K (1800° F) shows considerable data scatter. Therefore, the pressure effect can be obscured by the uncertainty in the mass loss measurements.

Plasma arc mass loss data obtained at the ARC and LaRC facilities are compared with data from tests performed in Rockwell and Vought Corporation radiant test facilities in figures 2(d) to 2(f). The mass loss data of figure 2(d) were obtained at an approximately equal RCC temperature (1233 K (1760° F) and 1256 K (1800° F)) and pressure (5.07 kN/m^2 (0.05 atmosphere)). The mass loss from specimens exposed in the plasma arc environment was approximately 30 to 50 percent higher than from specimens tested in a radiant environment for the same period. A comparison of this figure with figure 2(c)

again shows the effect of pressure on mass loss and the absence of any mass gain.

For RCC temperatures less than 1256 K (1800° F), both radiant and convective test results (ref. 1) indicate that little or no initial mass gain is experienced. Figure 2(e) is a comparison of mass loss at temperatures higher than 1256 K (1506, 1511, and 1536 K) and a pressure of 5.07 kN/m² (0.05 atmosphere). The significant difference between figures 2(d) and 2(e) is that figure 2(e) shows an initial mass gain for both the radiant and convective test specimens. The final slope of the mass loss data indicates a higher mass loss rate associated with the plasma-arc-tested specimens. Both figures 2(a) and 2(e) show that specimens exposed in a convective environment gained mass for a shorter time than did radiantly tested specimens. Figure 2(f) is a comparison of RCC mass loss in the temperature range of 1589 K (2400° F) to 1639 K (2490° F) and pressures of 1.01 kN/m² (0.01 atmosphere) to 7.60 kN/m² (0.075 atmosphere). At the low pressures (1.01 kN/m² (0.01 atmosphere) and 2.43 kN/m² (0.024 atmosphere)), no significant difference in performance between the radiant- and plasma-tested specimens is apparent based on the test duration. However, the mass gain period for the plasma-tested specimens again appears to be less than for the radiantly exposed specimens. The specimens tested at the higher pressures (5.47 and 7.60 kN/m²) in a convective environment have a shorter mass gain period and approach a constant final mass loss rate. This result contrasts with the comparable radiant specimen (6.67 kN/m²), which does not obtain as great a mass gain and appears to have reached its maximum mass gain after 2 hours of testing.

From the data presented in figures 2(a) to 2(f), two general observations are made. First, for a given exposure temperature and pressure, the final slope of mass loss exhibited by specimens exposed to a convective environment is higher than that exhibited by specimens exposed in a radiant environment. Second, at temperatures characterized by the initial mass gain phenomenon, the specimens exposed in a radiant environment have a longer duration mass gain period than do specimens exposed in a plasma arcjet facility.

The mass gain observed during the oxidation process is assumed to represent the difference between oxygen reacted to form silica and the mass of carbon lost by the reaction with oxygen. Stewart notes¹ that less fissure film growth appears to occur on the RCC coating during plasma arc exposures than during radiant exposures. Stewart suggests further that the difference between the film growth formation occurring in the radiant and plasma environments may be attributed to boundary-layer enthalpy and diffusion processes. Specifically related to these contributions are the differences in gas chemistry and fluid flow dynamics in the two types of facilities. A discussion of these effects is presented in the following section.

¹David A. Stewart (NASA Ames Research Center), personal communication, May 1975.

Effects of Gas Chemistry

As discussed in a preceding section, although the RCC has an oxidation-inhibiting SiC coating, the RCC material does lose mass over an extended temperature range without any apparent surface recession. Photomicrographs of the cross section of untested RCC specimens reveal a number of minute fissures in the coating, some of which traverse the coating and terminate at the coating/substrate interface. A photomicrograph of an RCC sample after exposure to a convective environment (fig. 1) shows the presence of voids at the coating fissure/substrate interface.⁴

Medford (ref. 2) postulated that oxygen diffuses through the SiC coating fissures to the substrate and reacts with the substrate; reaction products then diffuse back through the fissures to the free stream. Studies by Rosner and Allendorf (ref. 4) have indicated that the oxidation of SiC occurs in both an active (mass loss) and a passive (mass gain) regime. Reference 4 indicates that the active oxidation of SiC in diatomic oxygen (O_2) occurs in a region below a pressure-temperature locus of points from 1800 K, 1.33 kN/m², to 2000 K, 13.3 kN/m², and for oxidation in atomic oxygen (O), the pressures are 0.013 kN/m² and 1.33 kN/m², respectively. Rosner and Allendorf's results indicate that all the radiant and plasma arcjet facility test conditions lie above these loci of pressure and temperature, which would indicate that oxidation of the SiC coating occurs in a passive regime. This indication is further substantiated by the fact that no surface recession of the SiC coating was measured. Rosner and Allendorf (ref. 4), in their study of SiC oxidation over a temperature range of 1750 to 2400 K (2690° to 3860° F) at 1.33 kN/m² pressure, found that the SiC removal probabilities for both O and O_2 reactions displayed similar trends with temperature. For temperatures greater than 1900 K (2960° F), the O reaction probability was greater than the O_2 reaction probability; however, for temperatures less than 1900 K (2960° F), the O_2 reaction SiC removal probability exceeded that for the O reaction by an appreciable factor. These results further indicate that the difference in mass loss between the radiant and plasma arc testing cannot be attributed to SiC removal in the presence of dissociated gases.

The plots of cumulative mass change as a function of cumulative exposure time (figs. 2(a) to 2(f)) indicate that for temperatures greater than 1256 K (1800° F), there is an initial mass gain, attributed to coating oxidation, followed by a period of continuous mass loss. The mass gained during the coating oxidation process is assumed to represent the difference between oxygen reacted to form silica in the coating fissures and on the coating surface and the mass of carbon lost by reaction with the oxygen. At lower RCC temperatures, where apparently no protective silica layer is formed, there is continuous mass loss attributed to substrate oxidation. Therefore, it is

⁴Photomicrographs of RCC specimens after exposure to radiant environment also show voids at the coating fissure/substrate interface.

possible that dissociation associated with plasma arc testing enhances the oxygen diffusion to the substrate and/or that the oxidation of carbon for atomic oxygen is greater than for molecular oxygen and thus increases the substrate mass loss.

Rosner and Allendorf (refs. 5 and 6) studied the kinetics of graphite oxidation by dissociated gases. The results of these studies indicated that O atoms were significantly more effective than O₂ molecules in removing carbon atoms from the carbon matrix. Rosner and Allendorf's data indicate that the mass loss of carbon associated with an O reaction exceeded that associated with an O₂ reaction by an approximate factor from 200 to 7 as the graphite temperature varied from 1000 to 1600 K (1340° to 2420° F). Assuming dissociated oxygen at the RCC surface, it is necessary to establish the oxygen concentration profile down the fissure. Medford (ref. 2) found that the oxygen consumption by the fissure sidewalls was small compared to the oxygen diffusion rate down the fissures. Use of a characteristic recombination time developed by Rosner,⁵ which includes the O atom depletion associated with fissure sidewall recombination, indicated that sufficient time exists for the O atoms to penetrate the fissure depth by diffusion and reach the carbon at the base of the fissure. Neglecting wall recombination and using the gas-phase rate equations for dissociation-recombination of oxygen found in Vincenti and Kruger (ref. 7), an approximation of the time required for recombination of the O atoms was made. A comparison of this gas-phase recombination time with the flow time required for diffusion of the oxygen atoms across the coating indicated that atomic oxygen exists at the carbon substrate.

The previous paragraphs have indicated that the variation in RCC performance in the radiant and plasma arc test facilities appears to be explained by differences in gas chemistry. A significant remaining difference in the two facility environments is flow dynamics.

Effects of Flow Dynamics

The radiant tests were performed in a near-stagnant airflow, whereas the plasma arcjet provided a high-speed dissociated flow. The literature cited (refs. 4, 6, and 7) reflects tests performed in radiant heating facilities, which provided near-vacuum or low-flow-rate environments. It is highly probable that the high flow rate of a plasma arcjet provides a greater molecular and atomic oxygen concentration at the RCC coating surface, as well as at the subsurface oxidation site. The diffusional mass flux of an element can be expressed (ref. 8) as:

$$\dot{m}_{d_i} = \rho_e u_e C_{m_i} \left(\frac{\gamma}{k_{i_e}} - \frac{\gamma}{k_{i_w}} \right) \quad (1)$$

⁵D. E. Rosner (Yale University), personal communication, 1978.

Using the relationship between the heat- and mass-transfer Stanton numbers C_h and C_m suggested by Spalding (ref. 9) ..

$$\frac{C_m}{C_h} = L_e^{\gamma} \quad (2)$$

where γ is a constant, and assuming a Lewis number of unity, then

$$C_m = C_h \quad (3)$$

Combining equations (1) and (3), it follows that the increased heat-transfer coefficient associated with the plasma arc environment would result in a greater mass transfer of oxygen to the RCC surface, and thus to the carbon substrate, than would occur in the relatively static environment associated with radiant testing.

However, a calculated free convection mass-transfer coefficient associated with radiant testing is an order of magnitude higher than the mass-transfer coefficient associated with oxygen diffusion through the coating. This indicates that free convection alone is sufficient to prevent any significant reduction in the oxygen concentration at the RCC surface associated with the radiant tests.

The mass loss data shown in figures 2(a) to 2(f) indicate that the protective silica layer is removed sooner in the plasma tests than in the radiant tests at comparable temperature and pressure conditions. The early removal of this protective layer from within the fissures would increase the total fissure area and result in a higher substrate mass loss.

Based on the previous discussions, it appears that the increased mass loss associated with the plasma arc tests results from a combination of the dissociated gas state and early removal of the protective silica film.

MASS LOSS CORRELATION

The mass loss data discussed in the previous sections indicated that environmental characteristics, in addition to temperature and pressure, affect the performance of the coated RCC. The Space Shuttle Orbiter nose cap and wing panel outer skin locations are convectively heated, whereas the inner skin, rib, and attachment locations are heated by conduction and internal radiation in an almost stagnant airflow environment. Figure 3 is a photograph of a typical RCC wing panel; it illustrates the surface heated externally by forced convection of a dissociated gas and the radiantly heated internal surface, which is in a relatively static and predominantly molecular environment. This configuration indicates that mission mass loss prediction

correlations should be developed that are representative of the local environment associated with a specific RCC location.

By use of the mass loss rate data presented in tables I and II, subsurface mass loss correlations for both the radiant and the plasma arc test data were developed. An analytical model was developed analogous to that used in the analysis of bare carbon oxidation by Haviland and Medford (ref. 10), which included three oxidation control regimes: (1) the reaction control regime, in which surface chemical kinetics control oxidation rate, (2) the diffusion control regime, in which oxygen diffusion across the coating controls oxidation rate, and (3) the transition regime, in which both diffusion rate and surface kinetics are important. The subsurface mass loss data were empirically correlated by an equation similar to that of references 2 and 10 except for the assumption that two terms were needed to describe the observed data trend.

$$\frac{\dot{M}}{P^{0.8}} = \left(\frac{1}{\dot{M}_D} + \frac{1}{\dot{M}_{R_1}} \right)^{-1} - \left(\frac{1}{\dot{M}_D} + \frac{1}{\dot{M}_{R_2}} \right)^{-1} \quad (4)$$

Equation (4) can be rewritten as:

$$\frac{\dot{M}}{P^{0.8}} = \dot{M}_D \left(\frac{1}{1 + \frac{\dot{M}_D}{\dot{M}_{R_1}}} - \frac{1}{1 + \frac{\dot{M}_D}{\dot{M}_{R_2}}} \right) \quad (5)$$

where \dot{M}_D = diffusion limit

\dot{M}_{R_1} = reaction rate in reaction-rate-controlled region

\dot{M}_{R_2} = reaction rate in diffusion-controlled region

The reaction-rate-controlled mass loss was empirically correlated to temperature and pressure with the Arrhenius relation

$$\dot{M}_R = K e^{-\frac{E}{RT}} \quad (6)$$

where K is the reaction rate coefficient, E is activation energy, and R is the gas constant.

Substituting equation (6) into equation (5) yields

$$\frac{\dot{M}}{P^{0.8}} = \dot{M}_D \left(\frac{1}{1 + K'_1 e^{\frac{E_1}{R_1 T}}} - \frac{1}{1 + K'_2 e^{\frac{E_2}{R_2 T}}} \right) \quad (7)$$

where

$$K'_1 = \frac{\dot{M}_D}{K_1} \quad (8a)$$

and

$$K'_2 = \frac{\dot{M}_D}{K_2} \quad (8b)$$

The unknown coefficients in equation (7) (i.e., \dot{M}_D , E_1/R_1 , E_2/R_2 , K_1 , and K_2) were determined using the mass loss test data. The first term in the parentheses (eq. (7)) governs the mass loss rates for temperatures below 1367 K and the second term governs the mass loss rates above 1367 K. Equation (7) has been used to develop the mass loss correlations shown in figures 4 to 6. The radiant environment mass loss correlation is presented in figure 4 in terms of pressure-normalized mass loss rate as a function of inverse temperature. The corresponding convective environment mass loss correlation is shown in figure 5. A comparison of the mass loss data for both the radiant and the plasma tests (figs. 4 and 5) shows a data scatter over the RCC test temperature range. The 1256 K (1800° F) data, for instance, show a balanced number of data points from the radiant test occurring between 3.7×10^{-9} and $1.65 \times 10^{-8} \text{ kg/m}^2 \cdot \text{sec} \cdot (\text{N/m}^2)^{0.8}$. The plasma data all fall between 1.15×10^{-8} and $2.2 \times 10^{-8} \text{ kg/m}^2 \cdot \text{sec} \cdot (\text{N/m}^2)^{0.8}$ in the 1200- to 1300-K temperature range. For ease of comparison, the two correlations are plotted in figure 6. Figure 6 shows that for RCC temperatures of 1089 K (1500° F) to 1700 K (2600° F), the subsurface mass loss in a convective environment is 1.2 to 2.6 times the radiant environment mass loss.

The external surfaces of the Space Shuttle Orbiter nose cap and wing leading edges are exposed to a convective environment, whereas the internal areas are subject to a radiant environment; therefore, mission mass loss prediction correlations (such as those shown in fig. 6) should be used that are representative of the environments to which the specific RCC locations are analyzed. The RCC subsurface oxidation correlations (eq. (7) and fig. 6) and the entry trajectory provide the tools necessary to

make mission mass loss predictions. The RCC temperature and pressure profiles for each desired RCC location provide data inputs to the mass loss correlation functions. For example, a wing panel outer skin location would require the convective mass loss correlation, whereas a wing panel attachment location, which undergoes both conduction and radiant heating in an almost stagnant airflow environment, would require the radiant mass loss correlation. Localized mission mass loss is then determined by integrating the appropriate mass loss correlation over the entry trajectory profile. The amount of mass loss that can be accepted without structural concern should be established by structural performance tests, which determine the effect of mass loss on structural design properties and the limiting condition for mission life.

CONCLUDING REMARKS

A comparison of radiant and plasma arcjet effects on the mass loss history of silicon-carbide-coated reinforced carbon-carbon was made and possible reasons for the variations between the plasma arc and radiant test results discussed. Measured mass loss data from the plasma arc and radiant test facilities indicated greater mass loss associated with the plasma arc testing. It was also found that specimens exposed in a radiant environment have a longer duration mass gain period than do specimens exposed in a plasma arc facility. The final steady-state mass loss rate exhibited by specimens exposed to a convective environment was higher than that exhibited by specimens in a radiant environment at comparable temperature and pressure conditions. The most plausible explanation for the higher mass loss associated with the plasma tests is a combination of the dissociated test gas state and its effect on the substrate oxidation and of the early removal of the protective silica from the RCC surface.

Mass loss rate correlations have been developed with empirical constants determined from the available subsurface oxidation test data. Since the RCC surfaces of the Space Shuttle Orbiter are exposed to both convective (dissociated gas) and radiant (static molecular gas) environments, these types of correlations can be used to predict approximate RCC mass loss. A suggested method was given for predicting the mission mass loss for a particular RCC location.

Lyndon B. Johnson Space Center
National Aeronautics and Space Administration
Houston, Texas, May 23, 1978
953-36-00-00-72

REFERENCES

1. McGinnis, F. K.: Shuttle LESS Subsurface Attack Investigation Final Report. Report no. 221RP00241, Vought Corp., Dec. 1974.
2. Medford, J. E.: Prediction of Oxidation Performance of Reinforced Carbon-Carbon Material for Space Shuttle Leading Edges. AIAA paper 75-730, 10th Thermophysics Conference, 1975.
3. Medford, J. E.: Prediction of In-Depth Oxidation Distribution of Reinforced Carbon-Carbon Material for Space Shuttle Leading Edges. AIAA paper 77-783, 12th Thermophysics Conference, 1977.
4. Rosner, Daniel E.; and Allendorf, H. Donald: High Temperature Kinetics of the Oxidation and Nitridation of Pyrolytic Silicon Carbide in Dissociated Gases. J. Phys. Chem., vol. 74, no. 9, Apr. 30, 1970, pp. 1829-1839.
5. Rosner, Daniel E.; and Allendorf, H. Donald: High Temperature Kinetics of Graphite Oxidation by Dissociated Oxygen. AIAA J., vol. 3, no. 8, Aug. 1965, pp. 1522-1523.
6. Rosner, D. E.; and Allendorf, H. D.: Kinetics of the Attack of Refractory Materials by Dissociated Gases. Heterogeneous Kinetics at Elevated Temperatures, G. R. Belton and W. L. Worrell, eds., Plenum Press, 1970, pp. 231-251.
7. Vincenti, Walter Guido; and Kruger, C. H., Jr.: Introduction to Physical Gas Dynamics. John Wiley and Sons, Inc. (New York), 1965.
8. Moyer, C. B.; and Rindal, R. A.: An Analysis of the Coupled Chemically Reacting Boundary-Layer and Charring Ablator - Part II. NASA CR-1061, 1968.
9. Spalding, D. B.: Convective Mass Transfer. McGraw-Hill Publishing Co. (New York), 1963.
10. Haviland, J. K.; and Medford, J. E.: The Prediction of Oxidation Rates of Carbonaceous Materials From Plasma Arc Tests. Paper presented at 6th Biennial Conference on Carbon, June 17-21, 1963.

TABLE I.- RADIATIVE MASS LOSS CORRELATION DATA FOR 19-PLY BASELINE COATED RCC

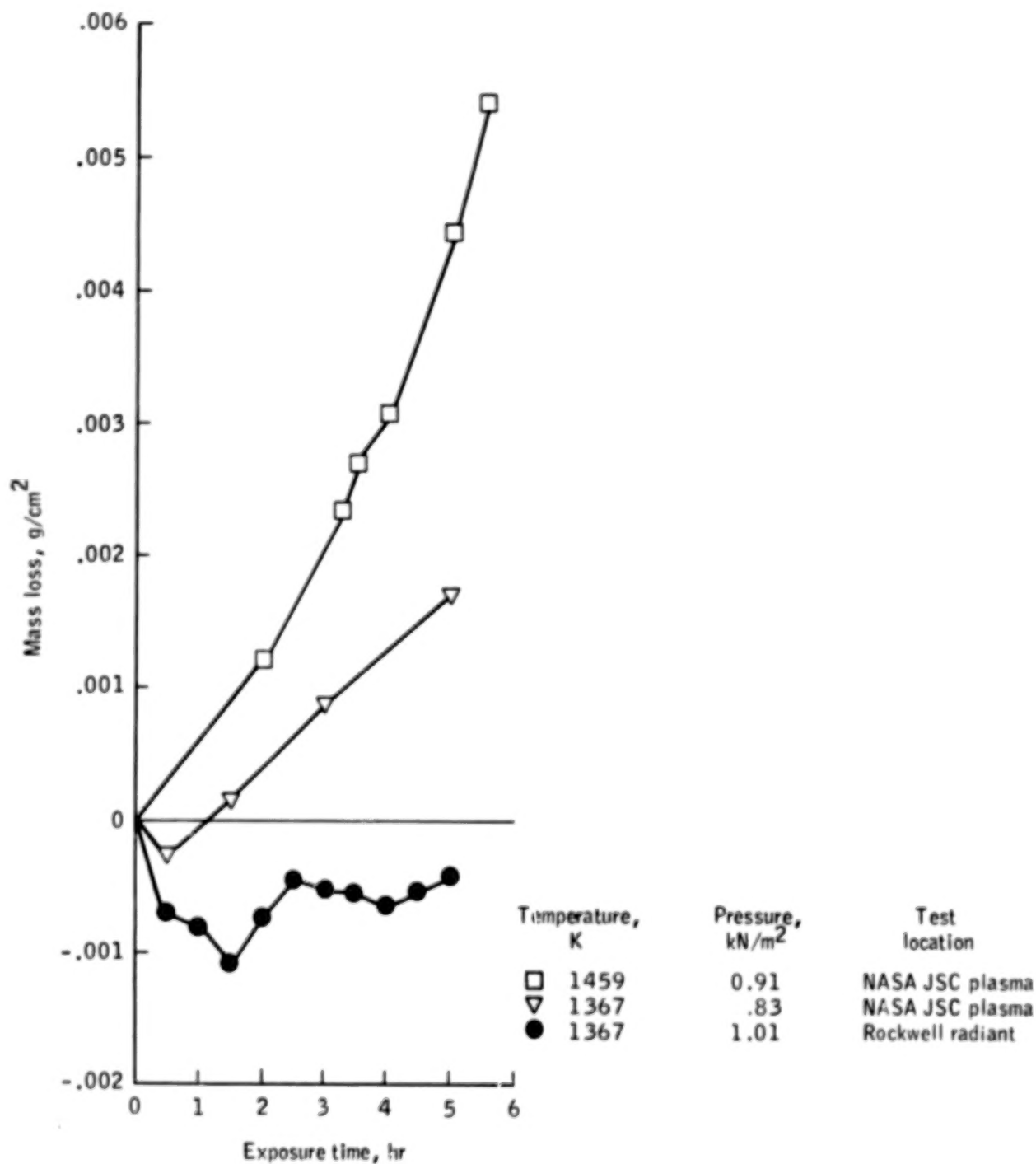
Radiant test facility	Temperature, K (°F)	Pressure, kN/m ² (atm)	Mass loss rate,	
			$\frac{\text{kg}}{\text{m}^2 \cdot \text{sec} \cdot (\text{N/m}^2)^{0.8}}$	$\left(\frac{\text{lbm}}{\text{ft}^2 \cdot \text{sec} \cdot \text{atm}^{0.8}} \right)$
Rockwell	922 (1200)	13.3756 (0.132)	4.699x10 ⁻⁹	(0.9726x10 ⁻⁵)
	922 (1200)	6.6878 (.066)	7.430	(1.538)
	922 (1200)	1.0133 (.010)	5.768	(1.194)
	1144 (1600)	13.3756 (.132)	9.228	(1.910)
	1144 (1600)	6.6878 (.066)	11.65	(2.411)
	1144 (1600)	1.0133 (.010)	9.682	(2.004)
	1256 (1800)	13.3756 (.132)	9.609	(1.989)
	1256 (1800)	13.3756 (.132)	7.479	(1.548)
	1256 (1800)	6.6878 (.066)	9.339	(1.933)
	1256 (1800)	6.6878 (.066)	10.76	(2.227)
	1256 (1800)	6.6878 (.066)	9.682	(2.004)
	1256 (1800)	6.6878 (.066)	8.430	(1.745)
	1256 (1800)	6.6878 (.066)	8.430	(1.745)
	1256 (1800)	6.6878 (.066)	10.59	(2.191)
	1256 (1800)	6.6878 (.066)	10.52	(2.178)
	1256 (1800)	6.6878 (.066)	10.10	(2.091)
	1256 (1800)	6.6878 (.066)	10.04	(2.079)
	1256 (1800)	6.6878 (.066)	10.21	(2.113)
	1256 (1800)	1.0133 (.010)	12.02	(2.488)
	1256 (1800)	1.0133 (.010)	16.81x10 ⁻⁹	(3.480x10 ⁻⁵)
	1256 (1800)	1.0133 (.010)	14.34	(2.969)
	1256 (1800)	1.0133 (.010)	13.75	(2.846)
	1256 (1800)	1.0133 (.010)	10.31	(2.133)
	1256 (1800)	1.0133 (.010)	10.94	(2.265)
	1256 (1800)	1.0133 (.010)	12.81	(2.651)
	1367 (2000)	6.6878 (.066)	4.037	(.8357)
	1367 (2000)	6.6878 (.066)	4.280	(.8860)
	1367 (2000)	1.0133 (.010)	6.493	(1.344)
	1478 (2200)	13.3756 (.132)	4.603	(.9527)
	1589 (2400)	6.6878 (.066)	3.493	(.7230)
	1700 (2600)	6.6878 (.066)	1.226	(.2537)
Vought mission cycle facility	1033 (1400)	10.133 (.10)	9.788	(2.026)
	1033 (1400)	10.133 (.10)	9.802	(2.029)
	1033 (1400)	10.133 (.10)	9.933	(2.056)
	1033 (1400)	10.133 (.10)	11.06	(2.289)
	1256 (1800)	5.0663 (.05)	5.459	(1.130)
	1256 (1800)	5.0663 (.05)	5.102	(1.056)
	1256 (1800)	5.0663 (.05)	4.637	(.9598)
	1256 (1800)	5.0663 (.05)	4.475	(.9263)
	1256 (1800)	5.0663 (.05)	3.777	(.7817)
	1506 (2250)	5.0663 (.05)	1.933	(.4000)

TABLE II.- CONVECTIVE MASS LOSS CORRELATION DATA FOR 19-PLY BASELINE COATED RCC

Plasma test facility	Temperature, K (°F)	Pressure, kN/m ² (atm)	Mass loss rate,	
			$\frac{\text{kg}}{\text{m}^2 \cdot \text{sec} \cdot (\text{N/m}^2)^{0.8}}$	$\left(\frac{\text{lbm}}{\text{ft}^2 \cdot \text{sec} \cdot \text{atm}^{0.8}} \right)$
NASA ARC	1714 (2625)	10.133 (0.10)	5.363x10 ⁻⁹	(1.110x10 ⁻⁵)
	1714 (2625)	10.133 (.10)	6.474	(1.340)
	1350 (1970)	5.5732 (.055)	14.88	(3.03)
	1350 (1970)	5.5732 (.055)	14.88	(3.08)
	1350 (1970)	5.5732 (.055)	17.49	(3.62)
	1233 (1760)	9.9303 (.098)	22.27	(4.61)
	1233 (1760)	9.9303 (.098)	13.33	(2.76)
	1089 (1500)	10.133 (.10)	13.67	(2.83)
	1089 (1500)	10.133 (.10)	12.85	(2.66)
	1233 (1760)	5.0663 (.05)	12.85	(2.66)
	1233 (1760)	5.0663 (.05)	13.09	(2.71)
NASA LaRC	1631 (2475)	5.4716 (.054)	3.821	(.791)
	1325 (1925)	1.1146 (.011)	11.21	(2.32)
	1414 (2085)	5.1676 (.051)	6.474	(1.34)
	1639 (2490)	7.9034 (.078)	2.646	(.5476)
	1633 (2480)	7.8020 (.077)	2.812	(.582)
	1339 (1950)	2.2292 (.022)	8.092	(1.675)
	1394 (2050)	4.9649 (.049)	6.860	(1.42)
	1608 (2435)	2.4318 (.024)	20.10	(4.16)
	1511 (2260)	5.0663 (.050)	6.909	(1.43)
	1547 (2325)	2.4318 (.024)	3.082	(.638)
	1608 (2435)	7.4980 (.074)	2.821	(.584)
NASA JSC	1589 (2400)	1.5199 (.015)	0.9595	(0.1986)
	1367 (2000)	1.0133 (.010)	4.635	(.9594)
	1756 (2700)	4.5599 (.045)	2.258	(.4673)
	1756 (2700)	4.4585 (.044)	2.028	(.4198)
	1447 (2145)	0.91197 (.009)	12.83	(2.655)
	1589 (2400)	2.3306 (.023)	1.906	(.3946)

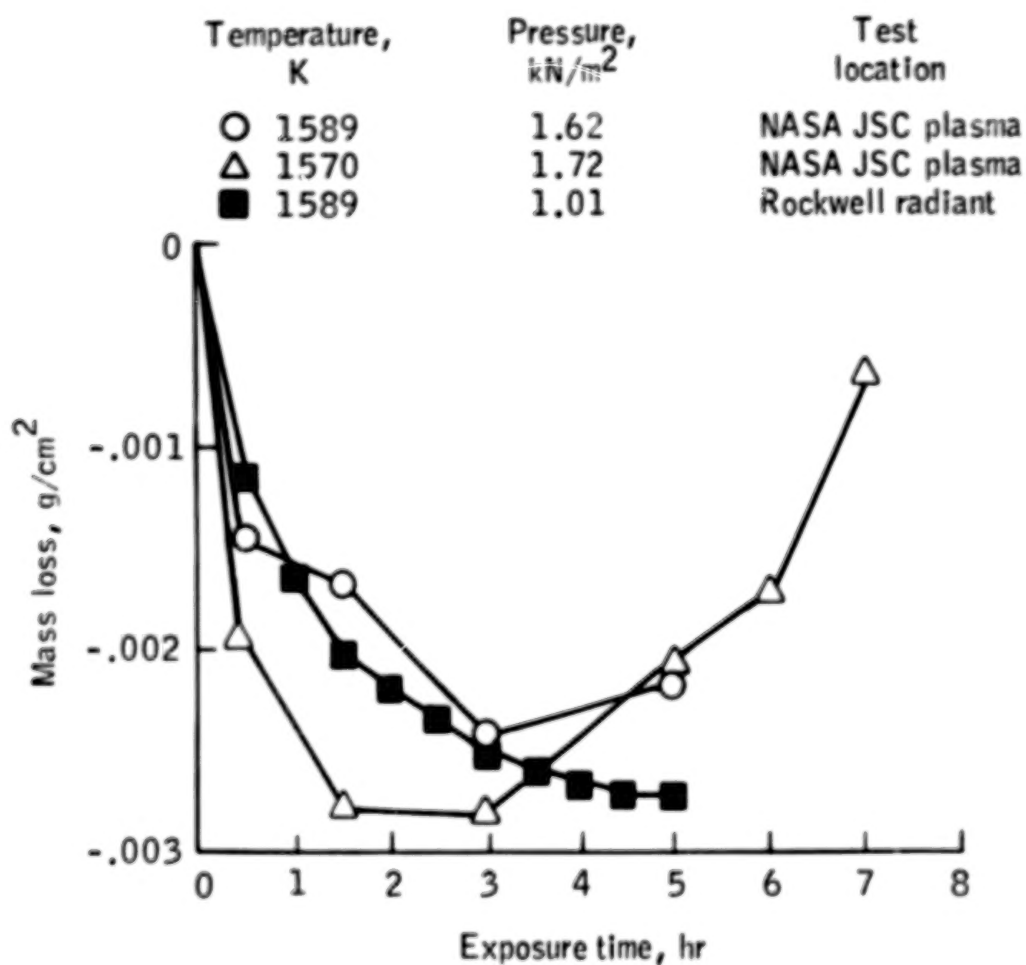


Figure 1.- Typical carbon-carbon substrate oxidation.



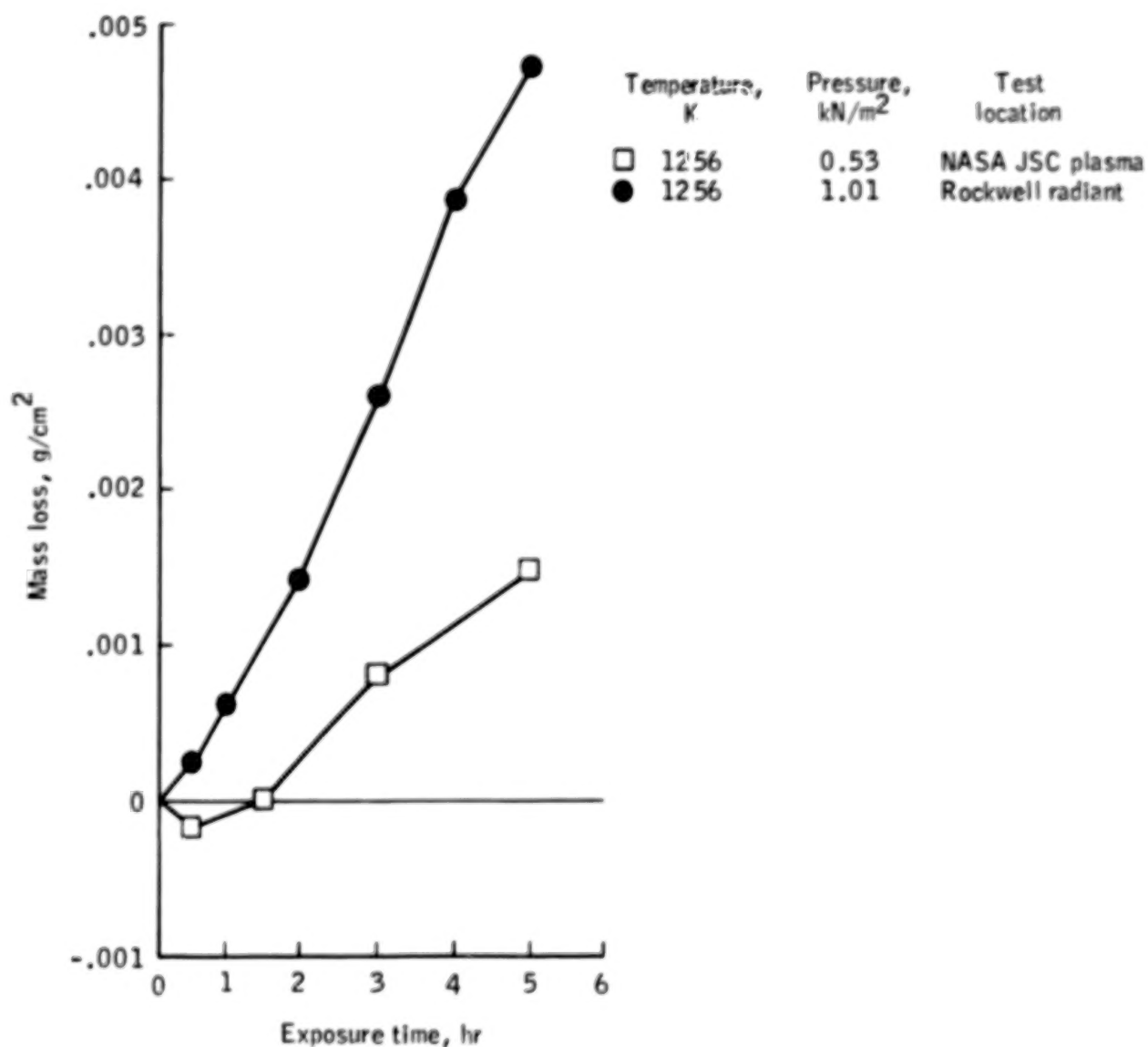
(a) At 1367 and 1459 K; 0.83, 0.91 and 1.01 kN/m².

Figure 2.- Coated RCC mass loss as a function of exposure time.



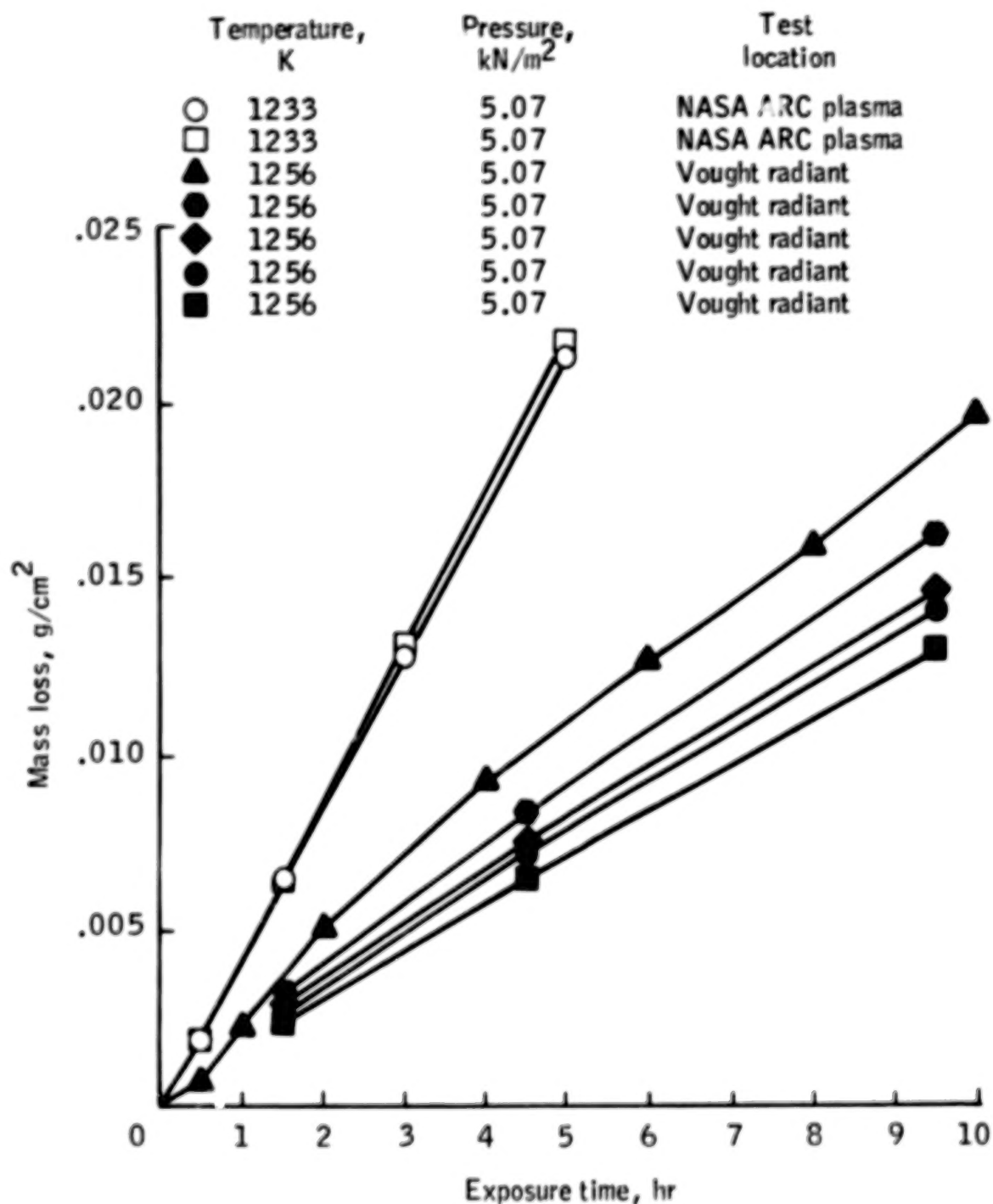
(b) At 1570 and 1589 K; 1.01, 1.62, and 1.72 kN/m².

Figure 2.- Continued.



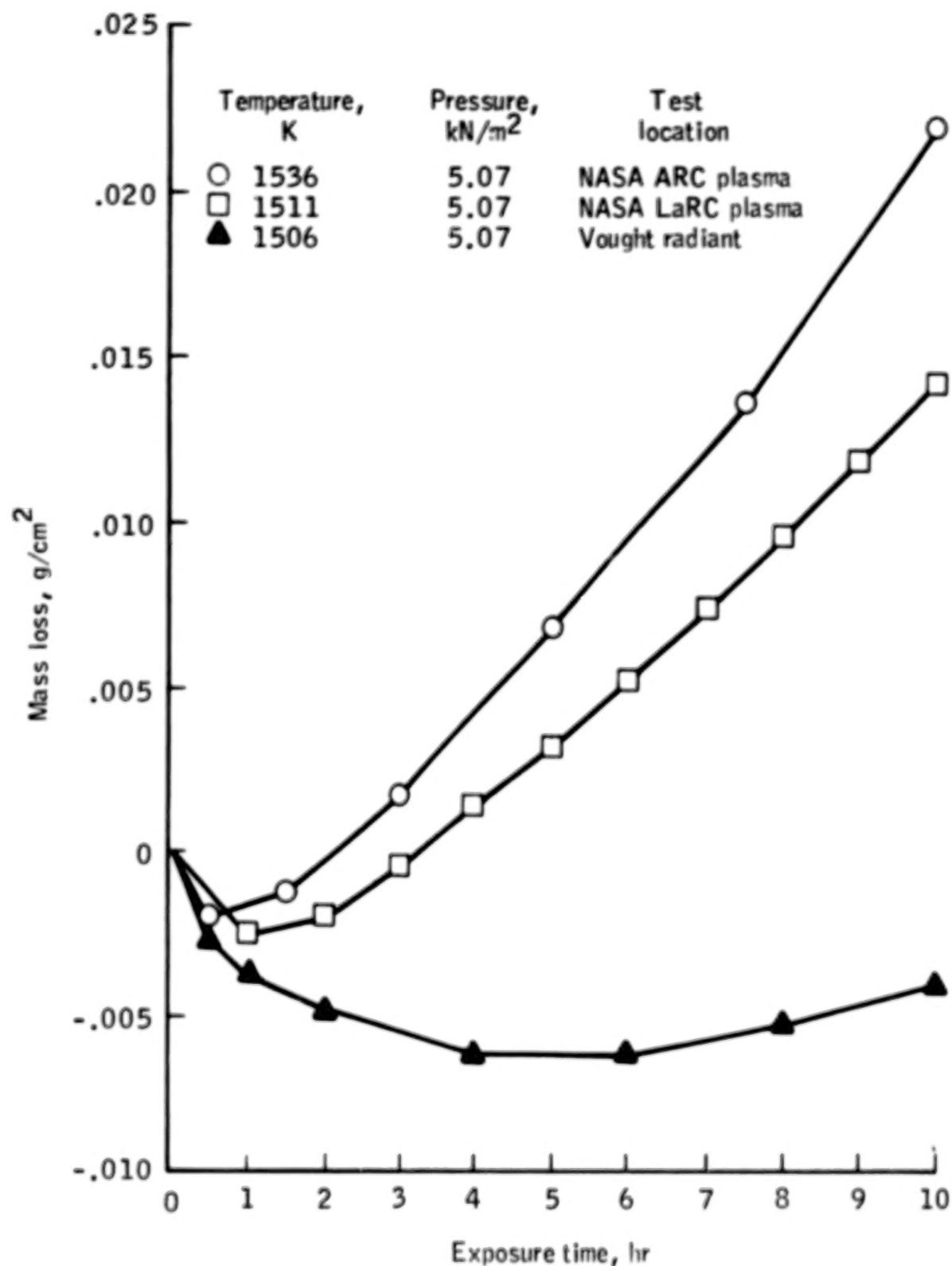
(c) At 1256 K; 0.53 and 1.01 kN/m².

Figure 2.- Continued.



(d) Ac 1233 and 1256 K; 5.07 kN/m².

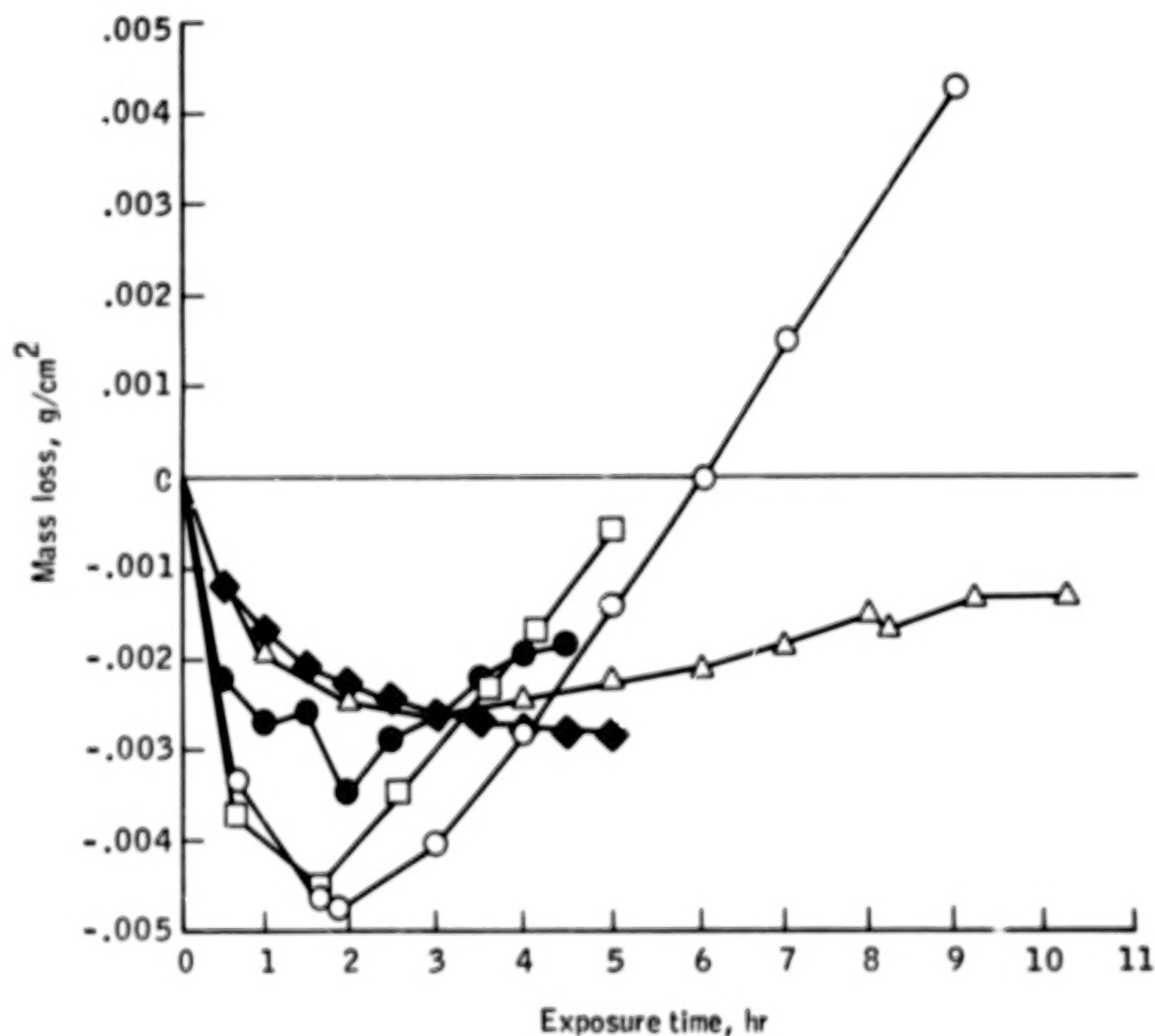
Figure 2.- Continued.



(e) At 1506, 1511, and 1536 K; 5.07 kN/m².

Figure 2.- Continued.

	Temperature, K	Pressure, kN/m ²	Test location
□	1639	7.60	NASA LaRC plasma
○	1631	5.47	NASA LaRC plasma
△	1608	2.43	NASA LaRC plasma
◆	1589	1.01	Rockwell radiant
●	1589	6.67	Rockwell radiant



(f) At 1589, 1608, 1631, and 1639; 1.01, 2.43, 5.47, 6.67, and 7.60 kN/m².

Figure 2.- Concluded.

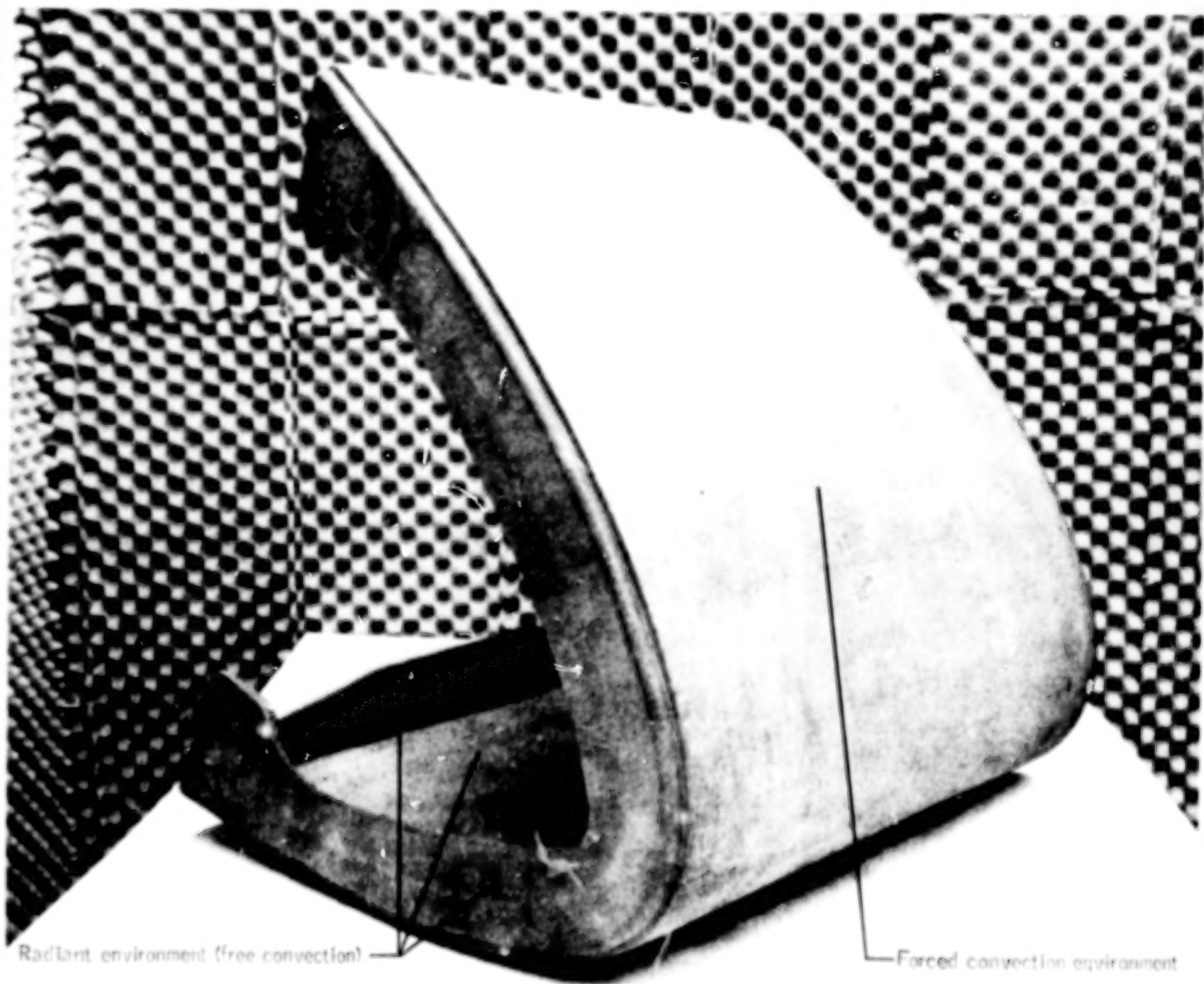


Figure 1. Type of RCU wing panel.

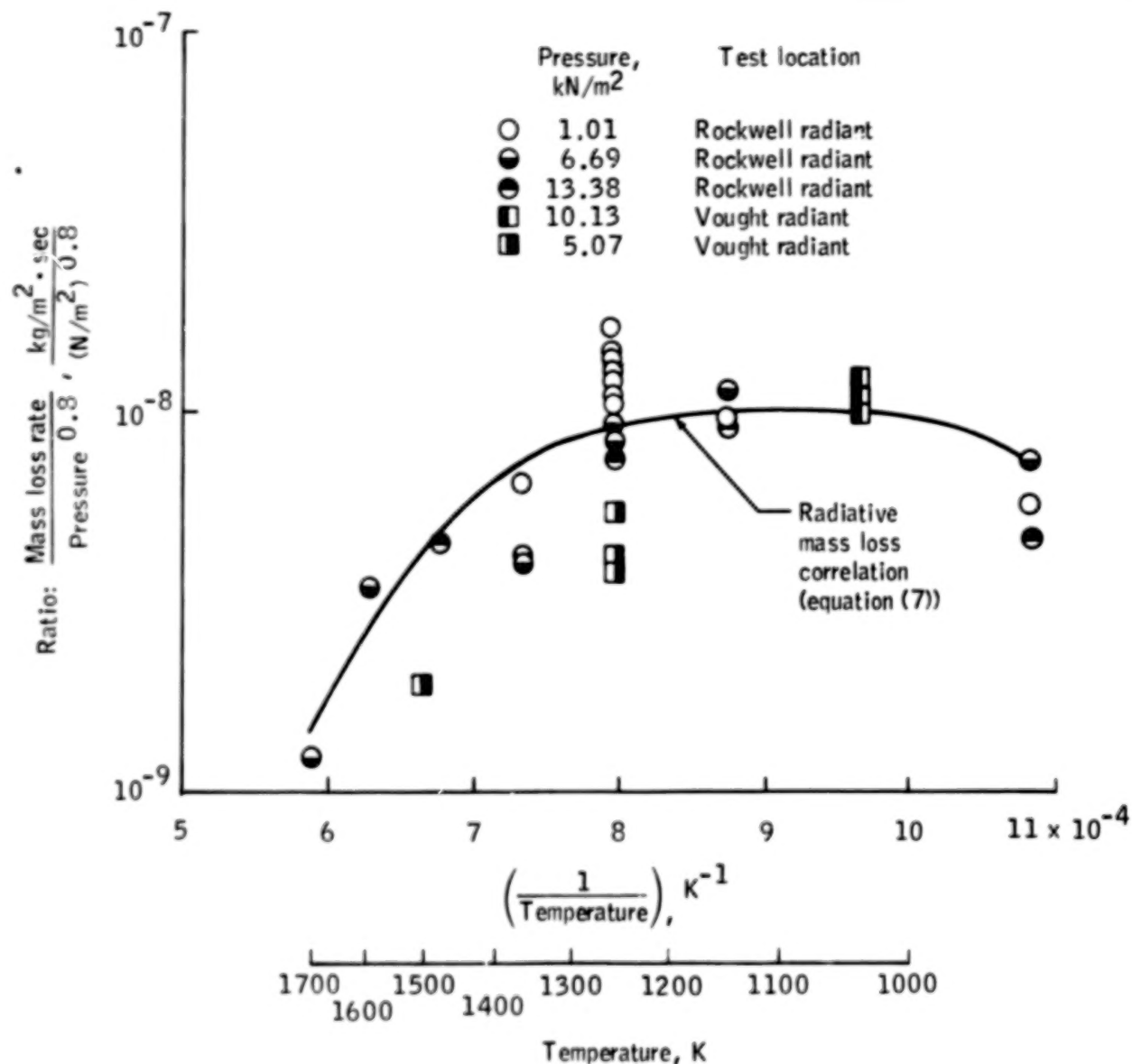


Figure 4.- Subsurface mass loss rate in a radiant environment.

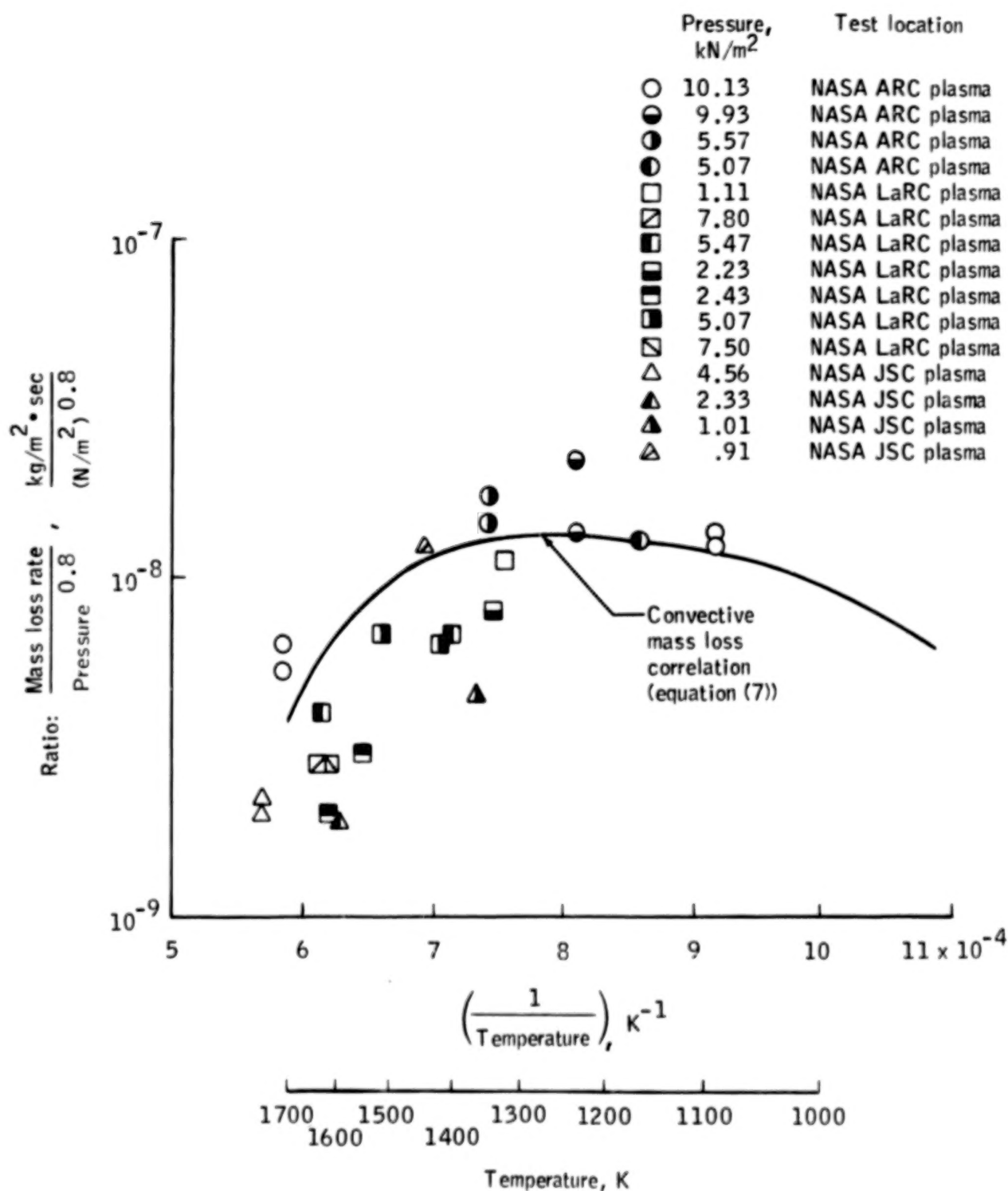


Figure 5.- Subsurface mass loss rate in a convective environment.

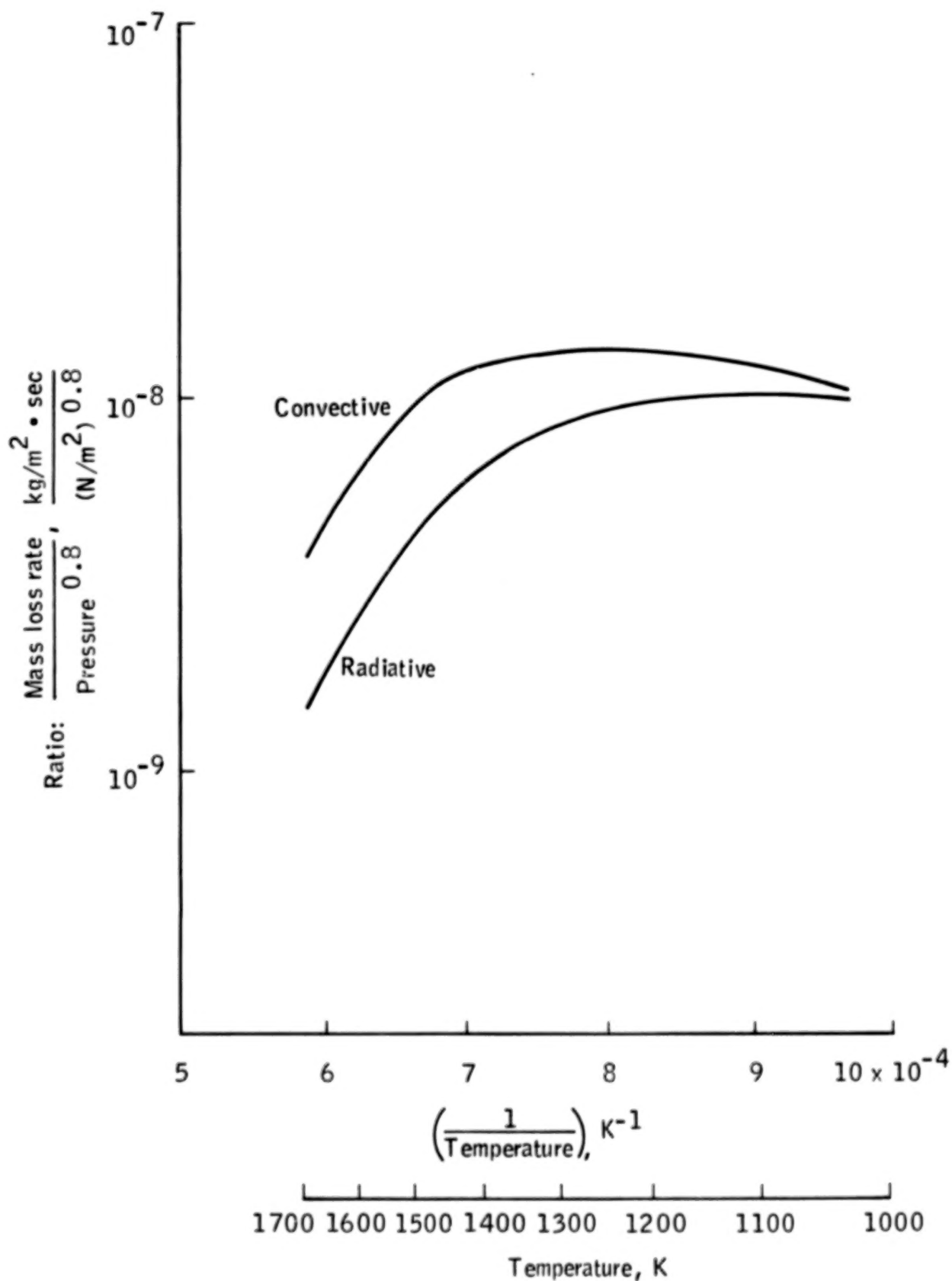


Figure 6.- Correlation of subsurface mass loss rates in radiative and convective environments.

1. Report No. NASA TP-1284		2. Government Accession No.		3. Recipient's Catalog No.	
4. Title and Subtitle REINFORCED CARBON-CARBON OXIDATION BEHAVIOR IN CONVECTIVE AND RADIATIVE ENVIRONMENTS				5. Report Date August 1978	
				6. Performing Organization Code	
7. Author(s) Donald M. Curry, JSC, K. J. Johansen, Vought Corporation, and Emily W. Stephens, JSC				8. Performing Organization Report No. S-485	
9. Performing Organization Name and Address Lyndon B. Johnson Space Center Houston, Texas 77058				10. Work Unit No. 953-36-00-00-72	
				11. Contract or Grant No.	
12. Sponsoring Agency Name and Address National Aeronautics and Space Administration Washington, D.C. 20546				13. Type of Report and Period Covered Technical Paper	
				14. Sponsoring Agency Code	
15. Supplementary Notes The second author, K. J. Johansen, is now with Shirco Corporation, Dallas, Texas.					
16. Abstract Reinforced carbon-carbon, which is used as thermal protection on the Space Shuttle Orbiter wing leading edges and nose cap, was tested in both radiant and plasma arcjet heating test facilities. In the test series described, conducted at varying temperatures and pressures, samples tested in the plasma arcjet facility had consistently higher mass loss than those samples tested in the radiant facility. A method using the mass loss data is suggested for predicting mission mass loss for specific locations on the Orbiter.					
17. Key Words (Suggested by Author(s)) Thermal protection Chemical reactions Carbon-carbon composites Silicon carbides Leading edges Space Shuttle Orbiters				18. Distribution Statement STAR Subject Category: 34 (Fluid Mechanics and Heat Transfer)	
19. Security Classif. (of this report) Unclassified		20. Security Classif. (of this page) Unclassified		21. No. of Pages 31	
				22. Price* \$4.00	

90

50

END

DEC 14 1978